Paper

Development of an Advanced Grid-Connected PV-ECS System Considering Solar Energy Estimation

Md. Habibur Rahman* Student Member
Susumu Yamashiro* Senior Member
Koichi Nakamura* Member

In this paper, the development and the performance of a viable distributed grid-connected power generation system of Photovoltaic-Energy Capacitor System (PV-ECS) considering solar energy estimation have been described. Instead of conventional battery Electric Double Layer Capacitors (EDLC) are used as storage device and Photovoltaic (PV) panel to generate power from solar energy. The system can generate power by PV, store energy when the demand of load is low and finally supply the stored energy to load during the period of peak demand. To realize the load leveling function properly the system will also buy power from grid line when load demand is high. Since, the power taken from grid line depends on the PV output power, a procedure has been suggested to estimate the PV output power by calculating solar radiation. In order to set the optimum value of the buy power, a simulation program has also been developed. Performance of the system has been studied for different load patterns in different weather conditions by using the estimated PV output power with the help of the simulation program.

Keywords: photovoltaic system, load leveling, electric double layer capacitor, energy capacitor system, distributed generation

1. Introduction

It is a great problem that, all over the world, the peak demand of load is increasing and the load factor of utility is decreasing year after year. A promising solution to this problem is distributed power generation system with load leveling function. Several works, both practical and simulation, have been done using PV panel and/or storage device in this regard [(1)(2)]. In this work, we have also developed a small grid connected distributed system with load leveling technique based on solar energy.

Photovoltaic power generation is spreading steadily and the desired PV panel is coming out from the architectural limitations, hence it is incorporated with our system to generate power from solar energy as a distributed system. EDLCs of large capacitance, called ultra or super capacitors, are used as energy storage device for their outstanding advantages [(1)]. Energy Capacitor System (ECS, now also renamed as ECaSS [(3)]), which is the combination of EDLCs and electronic circuits, can be charged and discharged quickly with high energy efficiency, has higher power density and longer lifetime and some other advantages over lead-acid battery. In our proposed system energy will be taken from grid line (hereafter will be called "buy power") and stored in EDLCs during the lower demand of load and will be supplied to load when its demand is high. Thus the system will keep the buy power as flat as possible (which is called load leveling). Moreover, it will generate power by PV panel during sunny days and supply to the load or charge the EDLC bank.

In this system we have to know, how much power will be taken from grid line tomorrow to level the load properly. To do that, it is important to know how much energy will be generated tomorrow by the PV panel. So a procedure has been developed to estimate the PV output power by calculating the solar radiation with the help of Hottel's and Liu-Jordan's equations [(4)].

For proper functioning of the system, it is necessary to declare the amount of tomorrow's buy power. It is not so easy to set the optimum value of this buy power for which the best result of load leveling will be achieved. To solve this problem, we have developed a program that can simulate the operation of the system. With the help of this simulation, the optimum value of buy power can be set by trial and error method.

Performance study of the system is being pursued to determine and to analyze the viability of the system, load leveling capability, the specific characteristics of ECS as storage device and the performance of PV panel as a renewable energy source. As we can now estimate the output power of PV panel and set the optimum value of buy power, better results are obtained than that of a previous work [(1)].

2. Description of the System

A simplified block diagram of the proposed system is shown in Fig. 1 and the brief description of each section is given in the following subheadings.

2.1 Load Unit The load, used in this system, is a resistive room heater of variable power, which consists of six resistive coils connected to the system by relays. The control unit can connect or disconnect the coils to the system by these relays as per requirement of the simulated load profile. The minimum value of this load is 50 W and the maximum value is 1150 W, but within this range the value can be set to any integer multiple of 50 W.

* Department of Electrical and Electronic Engineering
Kitami Institute of Technology
165 Koen-cho, Kitami 090-8507

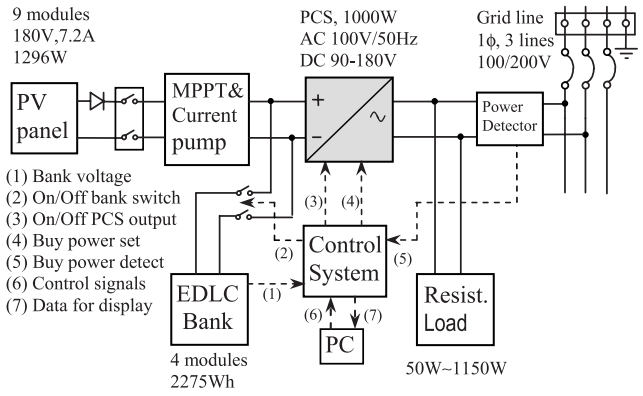

Fig. 1. Block diagram of the system

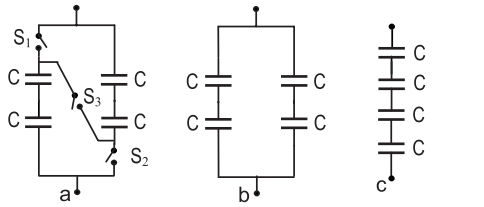

a. Switching circuit. b. Combination-I. c. Combination-II.

Fig. 2. Switching combinations of EDLC modules

2.2 PV Panel The PV modules consist of 42 solar cells connected serially where each cell has an area of 15 cm × 15 cm and can produce 0.6 V and 7.8 A of current at a specified standard condition (25 °C, Air mass 1.5 and Solar density 1 kW/m^2). The nominal open circuit output voltage of each module is 24.9 V and short circuit current is 7.69 A. The panel consists of 9 such modules connected in series. Its peak output power is 1296 W at MPP (Im=7.2 A Vm=180 V).

2.3 Energy Capacitor System It is the combination of super capacitors of very large capacitance like EDLC and electronic circuits. In our system the EDLC bank consists of four capacitor modules where each module comprises of 36 series connected EDLCs and seven such strings in parallel. The maximum voltage of each module is 90 V (2.5 × 36) and capacitance is 505.5 F (2600 F/cap. × 7 ÷ 36). The maximum capacitance of the combinations (Fig. 2) of the modules is 505.5 F and storage capacity is 2275 Wh ($1/2 \times 505.5 \times 180^2/3600$). To increase the storage capability and to yield a large energy output, electronic circuits called parallel monitors and current pumps, are used with the capacitors [5].

To keep the capacitor voltage within the input range of the Power Conversion System (hereafter will be called "PCS"), the modules are charged and discharged in two different combinations using switches S_1, S_2 and S_3 as shown in Fig. 2.

There were three combinations of the capacitor modules in a similar work done previously [1]. The additional combination was as shown in Fig. 3. It was necessary as the input voltage range of the previous inverter was 120 V to 180 V. But the input voltage range of the new PCS is 90 V to 180 V. Hence, this combination has been eliminated in the new system to reduce the number of switches that increases the efficiency of ECS.

2.4 Power Conversion System For a grid connected PV-ECS system, the inverter is very important. In this work,

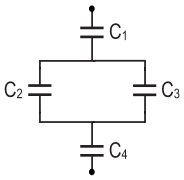

Fig. 3. Additional combination used in previous work

a very fast, low harmonic and efficient Error Tracking Mode Pulse Width Modulation (ETM-PWM) PCS [6] is used. It works as an inverter when power is supplied to load from ECS and PV panel, and as a charger when power is bought from grid line to charge the ECS. The dc input/output range of the PCS is 90–180 V and ac input/output range is 90–110 V 50 Hz. Using this PCS, we have eliminated the spikes appeared in the buy power curves of previous work due to the slow mode change action of the previous inverter [1].

2.5 Maximum Power Point Tracker (MPPT) To extract the maximum power from PV panel, an MPPT is used in our system. The MPPT always matches the dynamic impedance of PV panel with the fixed load. The microprocessor based MPPT, used in this system, has the maximum efficiency of 99% and capacity 1000 W.

2.6 Control Unit The control unit consists of an interfacing circuit as well as a data acquisition system. A microcomputer controls the entire system through the interfacing circuit. The data acquisition system (Agilent 34970 A) has an integrated type 20-bit ADC and can access data from 20 channels by time division multiplexing. It reads different data (like buy power, PV power, EDLC power, room temperature etc.) from the system and sends them to the computer. The control procedure is done with the help of a program, designed by LabView programming software.

3. Estimation of PV Output

The output power of the PV panel can be estimated if we know the amount of solar energy incident on it, efficiency of the panel and its area. So in this paper we have devised a procedure to calculate the daily solar energy for any day of the year, in any place, which is described in the following subheading.

3.1 Calculation of Solar Radiation in Kitami There are two components of solar radiation, one is beam radiation and the other is diffuse radiation. Solar radiation means the summation of beam and diffuse radiations. To calculate the beam radiation we have used Hottel's empirical formula of atmospheric transmittance for beam radiation [4], which is given below.

$$\tau_b = a_0 + a_1 e^{-k/\cos\theta_Z} \quad \cdots\cdots (1)$$

Where,

τ_b = Atmospheric transmittance for beam radiation (G_{bn}/G_{on})

G_{bn} = Beam radiation on the nth day of the year

G_{on} = Extraterrestrial radiation on the nth day of the year

θ_Z = Zenith angle

a_0, a_1 and k are constants; considering the weather of Kitami as mid-latitude winter and altitude 0.063 km the values of the constants have been calculated and found as 0.138344, 0.759559 and 0.381446 respectively (for mid-latitude summer these values are 0.130285, 0.744518 and 0.389075 respectively [4]).

The expression for extraterrestrial radiation [4] is

$$G_{on} = G_{sc}\left(1 + 0.033\cos\frac{360n}{365}\right) \cdots\cdots\cdots\cdots\cdots (2)$$

Where,

G_{sc} = Solar constant = 1353 W/m^2

n = Day of the year

Now multiplying Eq. (1) by Eq. (2) we get

$$G_{bn} = G_{sc}\left(1 + 0.033\cos\frac{360n}{365}\right) \times (a_0 + a_1 e^{k/\cos\theta z}) \cdots\cdots\cdots\cdots\cdots (3)$$

To calculate the value of G_{bn} for all the day we have to replace θz of Eq. (3) by local time of the place considered. For a horizontal surface $\theta z = \theta$ (incidence angle) and for inclined surface we have to use θz calculated for horizontal surface. There is a standard equation for the incidence angle [4], which is given below.

$$\cos\theta = \sin\delta\sin\varphi\cos\beta - \sin\delta\cos\varphi\sin\beta\cos\gamma + \cos\delta\cos\varphi\cos\beta\cos\omega + \cos\delta\sin\varphi\sin\beta\cos\gamma\cos\omega + \cos\delta\sin\beta\sin\gamma\sin\omega \cdots\cdots\cdots\cdots\cdots (4)$$

Where,

δ = Sun declination

ω = Hour angle

β = Slope of the surface

γ = Surface azimuth angle and

φ = Latitude of the place

Considering surface azimuth angle $\gamma = 0$ and slope of the surface $\beta = 0$ (as we will first develop an equation for horizontal surface), Eq. (4) reduces to

$$\cos\theta = \sin\delta\sin\varphi + \cos\delta\cos\varphi\cos\omega \cdots\cdots\cdots\cdots (5)$$

The values of these parameters are

δ = Sun declination = $23.45\sin\left(360\frac{284+n}{365}\right)$

φ = Latitude of Kitami = 43.75 °N

ω = Hour angle = $\frac{720\,\text{min} - slt(\text{min})}{4}$

slt = Solar time = Local time + $4(L_{st} - L_{loc}) + E$

E = Equation of time = $9.87\sin 2B - 7.53\cos B - 1.5\sin B$, $B = 360(n-81)/364$

L_{st} = Longitude based on which local time is calculated = 135 °E (for Kitami)

L_{loc} = Longitude of Kitami = 143.9 °E

Putting all these values into Eq. (5) we can get $\cos\theta$ in terms of local time and using this value into Eq. (3) we can calculate the beam radiation for any time of a particular day of the year. This value is plotted in Fig. 4. But from this curve we find that the radiation changes abruptly at sunrise and sunset time, whereas the practically measured solar radiation changes gradually. This error occurs due to the constant term in Hottel's equation (Eq. (1)) that does not depend on zenith angle θ_Z, i.e. due to this constant term some radiation will be available even at night which is not possible. Hence, to overcome this abrupt change, we have modified Hottel's equation by multiplying the constant term by an exponential function, which is related to zenith angle. The modified equation is shown below.

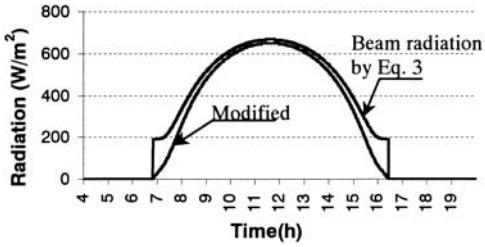

Fig. 4. Beam radiation on 31st January

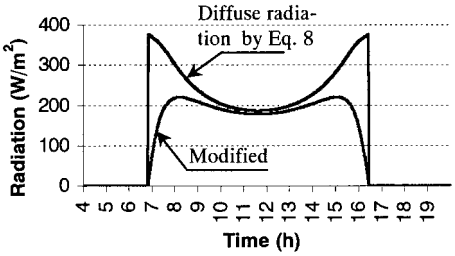

Fig. 5. Diffuse radiation on 31st January

$$G'_{bn} = G_{sc}\left(1 + 0.033\cos\frac{360n}{365}\right) \times \{a_0(1 - e^{-\xi_b\cos\theta z}) + a_1 e^{-k/\cos\theta z}\} \cdots\cdots\cdots (6)$$

Where, G'_{bn} = modified beam radiation, ξ_b = a constant = 5.

The value of the added exponential term is 0 at sunrise and sunset time but for other time of the day it is almost 1. So the modified equation produces almost the same beam radiation except during the sunrise and sunset time as shown in Fig. 4 (Modified curve).

To calculate diffuse radiation, we have used Liu and Jordan's empirical formula for the transmission co-efficient of diffuse radiation (τ_d) [4] that is given below.

$$\tau_d = 0.2710 - 0.2939\tau_b \cdots\cdots\cdots\cdots (7)$$

Multiplying Eq. (2) by Eq. (7) the clear sky diffuse radiation can be calculated as:

$$G_{dn} = G_{sc}\left(1 + 0.033\cos\frac{360n}{365}\right) \times (0.2710 - 0.2939\tau_b) \cdots\cdots\cdots\cdots (8)$$

Where, G_{dn} = diffuse radiation on the nth day of the year.

Fig. 5 shows the graph of this diffuse radiation that has also abrupt changes at sunrise and sunset time. So we have also

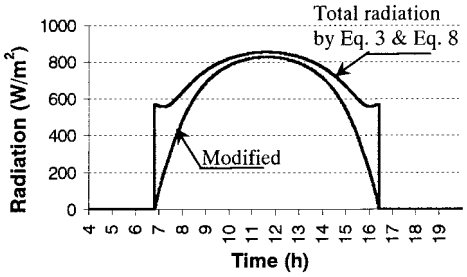

Fig. 6. Total solar radiation on 31st January

modified this empirical formula for τ_d in the same way as described for beam radiation. The modified equation is given below.

$$G'_{dn} = G_{sc}\left(1 + 0.033\cos\frac{360n}{365}\right) \times \{0.2710(1 - e^{-\xi_d \cos\theta_z}) - 0.2939\tau_b\} \quad \cdots\cdots (9)$$

Where, G'_{dn} = modified diffuse radiation, ξ_d = a constant = 8.

As shown in the graph of Fig. 5 (Modified curve), the modified equation changes the diffuse radiation only at sunrise and sunset time. The amount of energy lost (at sunrise and sunset time) depends on the value of the constant ξ_d. If the value of this constant is increased gradually the modified data will get closer and closer to the original value at sunrise and sunset time.

Finally, the solar radiation can be calculated by adding the beam and diffuse radiations as:

$$G'_{tn} = G'_{bn} + G'_{dn} \cdots\cdots (10)$$

Where, G'_{tn} = modified (total) solar radiation on the nth day of the year.

The solar radiation for 31st January has been calculated by modified equation (Eq. (10)) and by original equations (Eq. (3) & Eq. (8)), which are shown in Fig. 6.

3.2 Comparison of Calculated Solar Radiation with Practically Measured Radiation in Kitami Now we shall verify the accuracy of the calculated solar radiation by comparing it with practically measured solar radiation in Kitami. Solar radiation of Kitami has been measured for many years using a piranometer. For the purpose of comparison we have taken the data of 20 years. The problem is, although we have calculated the solar radiation for clear sky but the practically measured data is erratic due to cloudy effect. So we have sorted out the data to find out the clear sky radiation for every month of the year.

The solar radiation has been measured everyday in 17 time slots in one-hour intervals as shown in the Table 1 (here only the data for January 1994 is shown). The last row of this table contains the maximum value of each time slot. This maximum data is considered as the clear sky solar radiation for that month. Although it is likely to remain the sky clear once in a month in every time slot, practical results give different picture. So among 20 years we have got good results for 8-10 years for a particular month. Here, the data only for the month of January are shown (Fig. 7). It is note worthy form Fig. 6 and Fig. 7 that the practically measured solar radiation

Table 1. Measured solar radiation (W/m^2) in January (1994) in Kitami

4:0	5:0	6:0	7:0	8:0	9:0	10:0	11:0	12:0	13:0	14:0	15:0	16:0	17:0	18:0	19:0	20:0
0	0	0	0	0	55.5	425.6	219.4	218.5	186.6	486.9	517.5	82	0	0	0	0
0	0	0	0	0.7	46.4	476.8	563.1	448	413	24.9	11.2	38.7	0	0	0	0
0	0	0	0	60.2	266.9	342.1	235.1	238.4	203.7	141.9	0.6	0.3	0	0	0	0
0	0	0	0	169.7	469.7	565.6	202.7	532.2	623.5	217.2	107.9	0	0	0	0	0
0	0	0	0	0	0.2	38.9	86.2	646.8	782	366.3	110.7	123.1	0	0	0	0
0	0	0	0	1.4	186.7	384.6	573.3	756.6	699.5	492.2	323.3	53.5	0	0	0	0
0	0	0	0	0	0	0.3	34.2	340.1	0.5	75	56.7	1.7	0	0	0	0
0	0	0	0	203.1	479.8	700.9	749.3	747.4	706.1	502.5	316.1	110.8	0	0	0	0
0	0	0	0	7.9	268.5	474.6	484.6	334.8	395.4	245.6	14.3	2.7	0	0	0	0
0	0	0	0	191.9	502.8	449.6	755.2	684	307.3	520.8	112.9	123.8	0	0	0	0
0	0	0	0	3.5	8.3	40.7	170.3	143	126.3	546.6	426.6	104.2	0	0	0	0
0	0	0	0	129	493.4	663.2	714.4	637.1	543.1	213.3	118.5	19.1	0	0	0	0
0	0	0	0	1.3	48.8	151.5	583	733.2	501.3	280.7	156.6	54.1	0	0	0	0
0	0	0	0	80	525.9	661.9	717.2	724.5	709	603.7	107.7	133.7	0	0	0	0
0	0	0	0	31.1	36.1	186.7	352.9	799	645.1	199.1	203.8	303.1	0	0	0	0
0	0	0	0	108.2	165.5	270.2	206.1	46.3	16	107.8	206.6	31.3	0	0	0	0
0	0	0	0	0	0	0.3	0.4	4.8	21.2	155.6	3.2	0	0	0	0	0
0	0	0	0	0	9.3	94.1	401.3	154.5	168	404.4	475.4	163.7	0	0	0	0
0	0	0	0	185.3	361.5	180.5	115.3	91.3	18.6	39	0.7	0.2	0	0	0	0
0	0	0	0	144.4	512	673.1	736.5	735.1	544.7	398.1	369.1	247.5	0.8	0	0	0
0	0	0	0	261.4	591	727.4	775.7	805.2	794.1	739.3	614.5	303.4	0	0	0	0
0	0	0	0	0.2	5	575.3	748.6	767.8	730	713.7	584	277.5	1.9	0	0	0
0	0	0	0	7.1	0.3	0.5	0.3	0	0.8	258.4	582.3	293.9	1.5	0	0	0
0	0	0	0	236.4	567.7	706.5	760.6	793.6	718.8	640.5	555.6	87.2	0	0	0	0
0	0	0	0	285.1	458.7	586	363	351.7	228.3	65.8	162.2	143.9	0	0	0	0
0	0	0	0	0.5	35.4	292.5	336.1	337	473.4	182.9	134	82.4	0.5	0	0	0
0	0	0	0	0	3.5	7.1	70.3	7.2	213	406.3	108.8	0	0	0	0	0
0	0	0	0	6.1	367.5	638.1	732.8	746.3	517.5	84.1	250.8	262.1	10	0	0	0
0	0	0	0	274.4	505.9	657.4	460.9	658.3	752	722.3	608.1	273.5	5.1	0	0	0
0	0	0	0	0	1.9	233.7	49.2	0.7	0.4	0	0	0.2	0	0	0	0
0	**0**	**0**	**0**	**285.1**	**591**	**727.4**	**775.7**	**805.2**	**794.1**	**739.3**	**614.5**	**303.4**	**10**	**0**	**0**	**0**

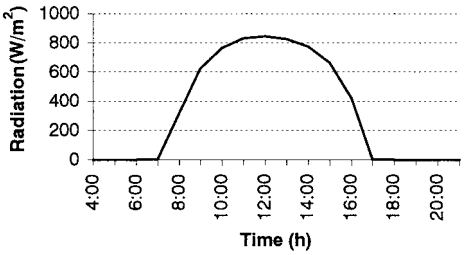

Fig. 7. Practically measured solar radiation in January in Kitami (average of 1988–1998)

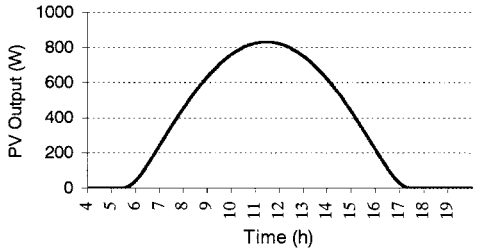

Fig. 8. Estimated PV output power on 11th April 2003

matches with the radiation calculated by the modified equation not with that calculated by the original equation. The integrated energy of the calculated radiation (using modified equation) is 5928 Wh/m^2 and that of the practically obtained radiations are 5645–6182 Wh/m^2, i.e. the calculated value is within the range of measured values.

3.3 Calculation of Output Power of PV Panel The total area of the PV panel installed in our site is 8.505 m^2 and its declination is 45 °S with azimuth angle 0°. Considering this declination, the solar radiation incident on the panel can be calculated by the above-mentioned procedure. Finally, the PV output power can be calculated by multiplying this value by the area and efficiency of PV panel and the efficiency of the MPPT. Considering panel efficiency 11% (at 25 °C with change of efficiency at a rate of −0.052%/°C) and MPPT efficiency 90%, the output power in a typical sunny day (11th

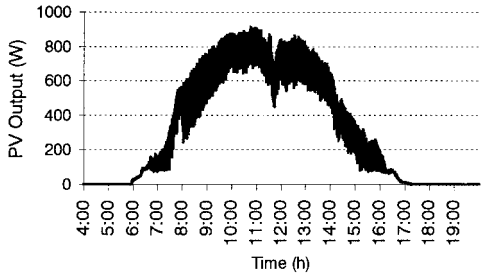

Fig. 9. Measured PV output power on 11th April 2003

April 2003) has been calculated and compared with the practically obtained value. These are shown in Fig. 8 and Fig. 9 respectively. The calculated PV output power is almost the same as the practically obtained output. To calculate the solar radiation and PV output power, we have considered sunny weather so far. But PV output power will also depend on the weather condition.

4. Operation Scheme of the System

The PV-ECS system works with an aim to level the load with the help of PV power and ECS power. In the daily operation of the system, emphasis is given to charge the EDLC fully at night when the price of power is low and to discharge it fully by day when the power is costly. This is important for the economical issue as described in section 7. The system is designed for load pattern of 1 kW maximum value. The peak energy (energy above the average power) of the load profile must be equal or less than the sum of PV and ECS energy. Since, the PV output energy is different for different months and also depends on weather condition, the peak energy of the load profile used in this work is kept fairly lower than this sum. The daily operation cycle of the system is shown in the flow chart of Fig. 10. Everyday the system starts at 7am. In every one-hour interval the value of the load (as given in the load pattern) and the buy power level will be set. If the load demand is greater than the buy power the additional demand will be met by EDLC power as well as PV output power if available. If PV power is not available, only EDLC power will do that. This type of operation is likely to occur by day. During night load demand will be lower than the buy power. So the extra buy power will be used to charge the EDLC. In this way, the system will perform the function of load leveling by taking always the same amount of buy power.

5. Performance Study of the System

To study the performance of our system, three load profiles have been simulated and the performance has been studied in different weather conditions for several days. The load profiles and the methodology used for performance study are described below.

5.1 Load Profiles Fig. 11 depicts the designated specific profiles of loads simulated by the resistive room heater. Among these load patterns, first two (Fig. 11(a) & (b)) are hypothetical and the last one (Fig. 11(c)) is a typical residential load pattern. In the first load, the peak demand is from 11:00 am to 12:00 pm and although the demand during daytime is very high but is very low during night. In the second load, the peak demand is from 12:00 pm to 1:00 pm. Compared

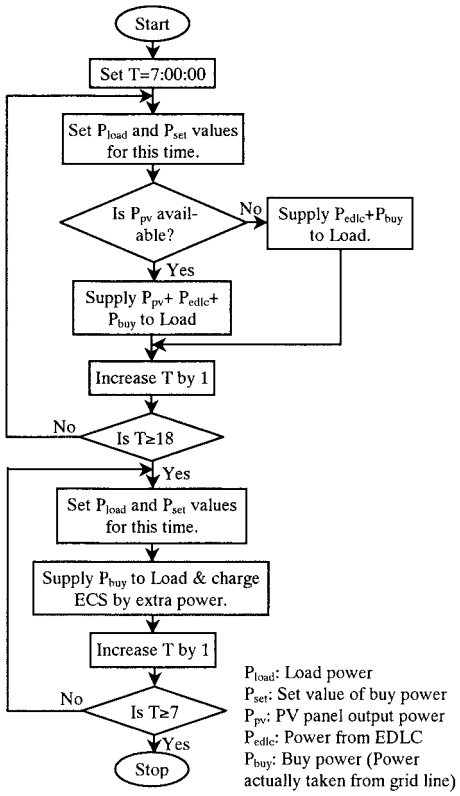

Fig. 10. Flow chart of daily operation of the system

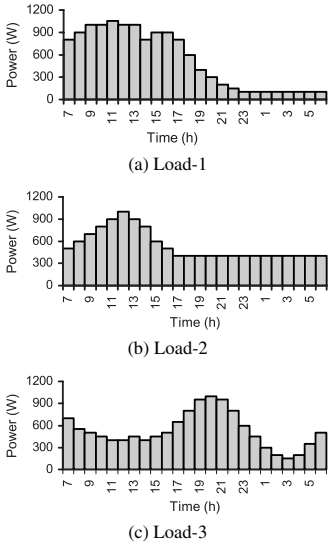

(a) Load-1

(b) Load-2

(c) Load-3

Fig. 11. Load profiles

to the first load, here the demand by day is lower but higher at night. On the other hand load-3 has lower demand by day and higher demand at evening and at night the demand is even lower than daytime. The average power, total energy, load factor (LF: ratio of average load to maximum load) and load form factor (LFF: the ratio of the total energy above the average power to the daily total energy) of each load profile are given in Table 2.

5.2 Calculation of Buy Power Although for a sunny day it is possible to estimate the PV output power, it is not so easy to calculate the optimum value of buy power. We can try to find this value considering the following equation.

Table 2. Parameter values of load profiles

Load	Average Power (W)	Total Energy (kWh)	LFF (%)	LF (%)
Load – 1	525.0	12.6	35.32	50.0
Load – 2	537.5	12.9	15.46	53.75
Load – 3	529.17	12.7	17.56	52.92

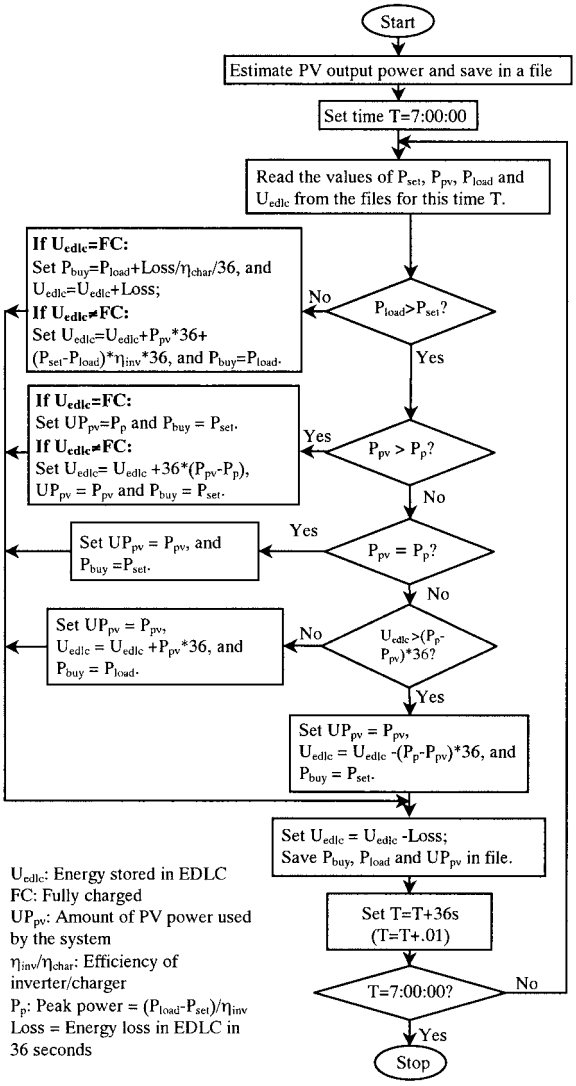

Fig. 12. Flow chart of the simulation program

$$\text{Total } U_{load} + \text{Total Loss} = \text{Total } U_{buy} + \text{Total } U_{pv} \quad \cdots\cdots\cdots\cdots\cdots\cdots (11)$$

Where,

U_{load} = Energy consumed by load

U_{buy} = Energy of buy power

U_{pv} = Energy produced by PV panel

Total Loss = Loss of the whole system

The energy of the EDLC is not included in this equation since it will be discharged during day and charged during night. We need the hour by hour values of buy power to get the optimum results of load leveling, not only the total/average value that can be calculated by Eq.(11). To overcome this difficulty, a simulation program has been developed that can simulate the operation of the system. The flow chart of this program is shown in Fig. 12. First, the program will be run by setting an arbitrary value of buy power. It will estimate the PV output of the day and simulate the operation of the system using the estimated PV output and the set value of buy power. If this value of buy power is lower than the optimum value, EDLC will be fully discharged before the expected time by day. So we will set higher value of buy power and run the program again. But if the value is greater than the optimum value, EDLC will be fully charged before the desired time at night. Hence, we will set lower value of buy power and run the program again. In this way, the optimum value of buy power can be determined by trail and error method for which better load leveling is possible.

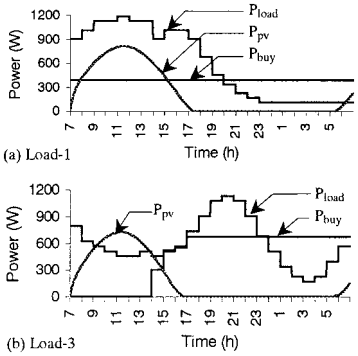

Fig. 13. Simulated power flow patterns in typical sunny days

The power flow patterns simulated by this program for load-1 and load-3 in a typical sunny day are shown in Fig. 13. Since, the performance of the system depends on the PV output power and the load pattern, for load-1 buy power is flat for all day but for load-3 it is not flat. But considering the limit of our EDLC and the daily operation scheme (EDLC fully charged at night and fully discharged by day) this is the optimum result. Using this program, the optimum values of the buy power have been calculated by trial and error method. To set the buy power for sunny day, PV output has been calculated as described in section 3.3, but for cloudy day, since we didn't have a means to calculate this value correctly yet, it has been assumed to be zero in this paper to ascertain that the load leveling function can also be realized even in cloudy weather.

6. Results and Discussion

Fig. 14 and Fig. 15 represent the performance of power flow in the system for some typical sunny days and cloudy days. The graphs show the power consumed by load (P_{load}), power produced by PV panel (P_{pv}) and the buy power (P_{buy}). If we compare the powers consumed by the loads with the simulated load profiles (Fig. 11) we find that the consumed powers are a little bit greater than the simulated powers, and there are some fluctuations. Explanation of this discrepancy is, the resistance of the load is fixed considering the line voltage 100 V, but the line voltage to which the system is connected is greater than 100 V and there are some fluctuations. For this reason the variation occurs in the powers actually consumed by the loads.

Observing the powers generated by PV panel in sunny days

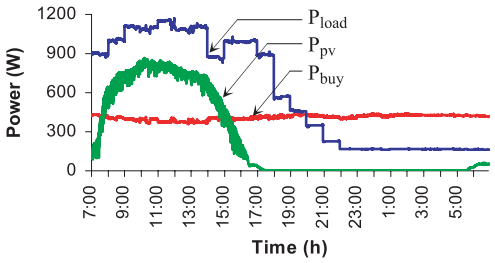

(a) Load-1

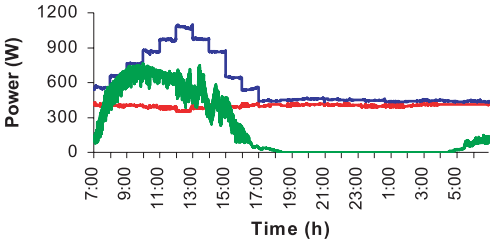

(b) Load-2

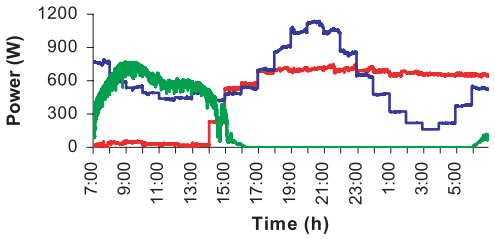

(c) Load-3

Fig. 14. Power flow patterns in the system in sunny days

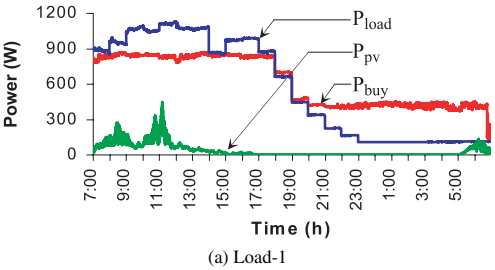

(a) Load-1

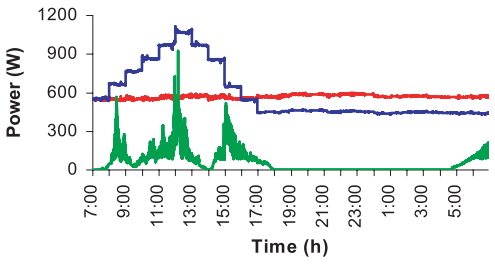

(b) Load-2

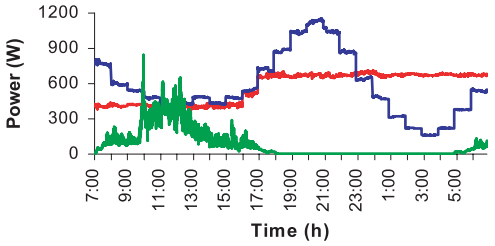

(c) Load-3

Fig. 15. Power flow patterns in the system in cloudy days

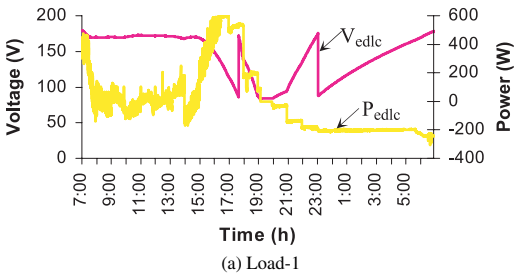

(a) Load-1

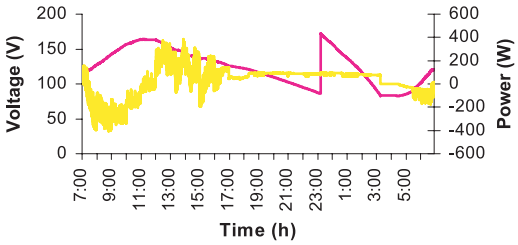

(b) Load-2

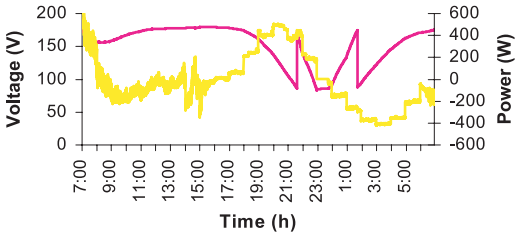

(c) Load-3

Fig. 16. Charging and discharging patterns of EDLC in sunny days

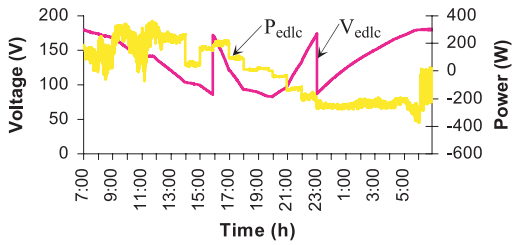

(a) Load-1

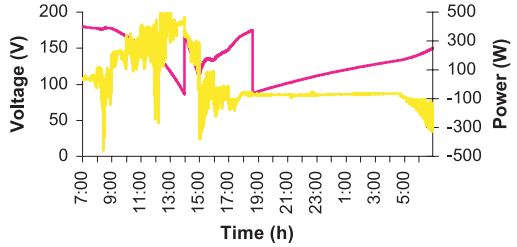

(b) Load-2

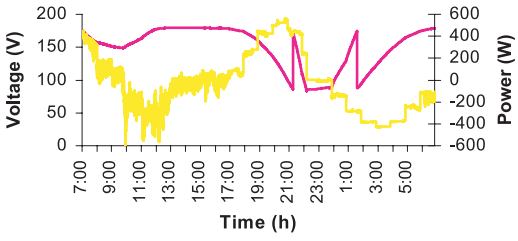

(c) Load-3

Fig. 17. Charging and discharging patterns of EDLC in cloudy days

we find that, for laod-1 and load-2 (Fig. 14(a) & (b)), 100% of these powers have been used by the system and the buy powers remain flat. But for load-3 (Fig. 14(c)), although 100% of PV output power has been used, it is not possible to keep the buy power flat for all day long, as the peak of the load is shifted from the PV panel's generation time. This problem can be overcome by increasing the capacitance of ECS by 1900 Wh. For cloudy days, we find different power flow patterns but the load powers are same. The output power of the PV panel is very low and hence we have to take more buy power compared to the sunny days. Although it is possible to level the buy power for all day long for load-2 (Fig. 15(b)), but due to the higher demand of load-1 and lower demand of load-3 during daytime, it is not easy to level the buy power properly. This problem can be solved by increasing the capacitance of ECS by 2175 Wh and changing the daily operation scheme.

In a previously designed system, due to the relatively slow operation mode change of the inverter, there were spikes in the buy power curves [1] but in our present system, since the PCS is very fast, there are no such spikes. The performance of the system as load leveler is summarized in Table 3 and the efficiencies of different units are shown in Table 4.

The charging and discharging patterns of the EDLC in sunny and cloudy days are shown in Fig. 16 and Fig. 17 respectively. Here, V_{edlc} and P_{edlc} represent the terminal voltage and charge-discharge power of EDLC bank respectively. The charging and discharging patterns of load-1 (Fig. 16(a) and Fig. 17(a)) are same, fully discharged during day and fully charged during night (it is important for economical issue as described in section 7). For load-2, the EDLC is fully charged and discharged in cloudy day but not in the sunny day. It is possible to do that also for sunny day but the buy power will not be so flat in that case. Again, the charging and discharging patterns of load-3 (Fig. 16(c) & Fig. 17(c)) show that the EDLC is fully charged at night and fully discharged in the evening both in sunny and cloudy days. Charging and discharging efficiencies are also shown in Table 4. We have tried to run our system to get maximum load leveling and economic benefit by charging the EDLC fully at night and discharging it fully during day. But, fully charging and discharging of EDLC is not possible for some situations (Fig. 16(b)) for the sake of load leveling. However, for non-flat price of electricity (price of electricity in peak hours is greater than that of off-peak hours) the system will be more economical for users if the EDLC is fully charged during off-peak hours and fully discharged during peak hours instead of leveling the load for all day long.

The daily efficiencies of different units, calculated as the ratio of daily total energy supplied by the unit to the daily total energy taken by it, are shown in Table 4. From this table, we find that the highest efficiencies of MPPT, PCS(inv) (PCS when works as an inverter), PCS(char) (PCS when works as a charger) and EDLC are 98.5%, 92.5%, 81.4% and 89.3% respectively in sunny days and in cloudy days these are 92.3%, 85.2%, 78.5% and 89.7%. In case of PCS, actual efficiencies are higher than the values shown here, since the current pump and other sensing circuits consume some power. Also the charging and discharging efficiencies of the EDLC are higher than the obtained values, since the sensing and switching circuits in the EDLC consume some power. For some load patterns the efficiencies of PCS(char) and the EDLC have not been calculated, since for these loads the EDLC was not charged and discharged fully (efficiency of EDLC and PCS(char) can't be calculated accurately if EDLC is not fully charged and discharged). The overall efficiency (calculated as: $(P_{laod} - P_{direct})/(P_{pv} + P_{buy} - P_{direct})$, where P_{direct} is the power supplied by grid line directly to the load) calculated for Load-1 is 82%.

Table 3. Comparison of LFF and LF with and without PV-ECS system

Days	Items	Load-1	Load-2	Load-3
Sunny day	LFF without PV-ECS	32.5%	14.73%	17.93%
	LFF with PV-ECS	**1.8%**	**1.3%**	**29.3%**
	LF without PV-ECS	50.5%	53.78%	50.5%
	LF with PV-ECS	**93.1%**	**93.63%**	**61.67%**
Cloudy day	LFF without PV-ECS	35.0%	14.56%	18.04%
	LFF with PV-ECS	**16.6%**	**0.93%**	**10.74%**
	LF without PV-ECS	50.2%	53.07%	50.15%
	LF with PV-ECS	**71.5%**	**95.44%**	**80.30%**

Table 4. Daily efficiencies of different units of the system

	Efficiency of	Load-1	Load-2	Load-3
Sunny day	MPPT	98.5%	97.4%	98.5%
	PCS (inv)	92.5%	82.6%	87.6%
	PCS (char)	81.4%	-	74.4%
	EDLC	89.3%	-	84.5%
Cloudy day	MPPT	92.3%	91.7%	97.3%
	PCS (inv)	85.2%	84.3%	77.8%
	PCS (char)	78.5%	54.3%	77.2%
	EDLC	89.7%	--	77.5%

7. Economical Issues

Although the main object of this system is to level the buy power, it will also provide a superb financial benefit. It can help the user to save money in two ways. First one is, during sunny days the system can generate power by PV, which is used for load without any cost. The second one is, it can charge the EDLC bank by cheaper power during night and can use this power to fulfill the load demand during day when the price of power is very high. Thus, the system can help the users to use cheaper power instead of costly one. The financial benefit in the operating days, for which results have been described in this paper, has also been calculated and shown in Table 5. Benefit has been calculated considering both flat price of electricity (Unit price of electricity in peak hours R_p = that in off-peak hours R_o) and non-flat price of electricity ($R_p = \alpha R_o$, $\alpha \neq 1$). Although for different load patterns, duration of peak hours and off-peak hours should be different, for simplicity we have assumed 7am to 19pm as peak hours and 19pm to 7am as off-peak hours and $\alpha = 1.6$, which is a threshold value to overcome the loss in cloudy days. From Table 5, we find that for flat price maximum saving of $4.52R_o$ is possible using the system in sunny days. But for cloudy days saving is very low even sometimes the

Table 5. Savings using the system

Days	Price Type	Savings		
		Load-1	Load-2	Load-3
Sunny day	Flat price (R_p=R_o)	4.38 R_o	4.52 R_o	2.73 R_o
	Non-flat price (R_p=1.6R_o)	**8.54** R_o	**6.94** R_o	**5.07** R_o
Cloudy day	Flat price (R_p=R_o)	-1.3 R_o	.55 R_o	.02 R_o
	Non-flat price (R_p=1.6R_o)	**00** R_o	**1.83** R_o	**.95** R_o

R_p = Unit price of electricity in peak hours
R_o = Unit price of electricity in off-peak hours

system may provide loss (Table 5, Load-1). For non-flat price of electricity, maximum saving is 8.54R_o in sunny days and 1.83R_o in cloudy days. So from this result we can say that for flat price of electricity the system is economically beneficial in sunny days but not in fully cloudy/rainy days. On the other hand, for non-flat price of electricity ($\alpha \geq 1.6$) the system is profitable both in sunny days and cloudy days.

Although the price of PV panel and super capacitors is very high now, manufacturers are trying to reduce their costs. So if the price of the necessary components of the system goes down considerably, our system will help the users to save the expenditure for power.

8. Conclusion

As shown in Table 3, the LFFs with PV-ECS are smaller than those without PV-ECS and the LFs with PV-ECS are higher than those without PV-ECS in sunny and cloudy days for all of the three load patterns (except for Load-3 in sunny day). Hence, we can say that the system works as a good load leveler. The enhancement of LFF and LF by the PV-ECS depends on the power generated by PV panel and the preset buy power. As we can estimate the power generated by the PV panel in sunny day, it is possible to make the buy power very flat (good load leveling system). But for the partially cloudy days it is not easy to make the buy power flat properly due to the difficulty to estimate the PV output power correctly. Again the improvement of LFF and LF depends on the load pattern and for some load patterns it is not possible to level the buy power even in sunny day (Load-3 of Fig. 14), if we want to use maximum output of the PV panel and to charge the EDLC fully at night and discharge by day. For this load pattern we can level the buy power properly but all of the PV output will not be used by the system. By changing the operation scheme of the system and increasing the capacitance of the ECS this problem can be solved as mentioned earlier.

Finally, we conclude that the efficiency of the system has been increased by 8% (efficiency of the present and previous system is 82% and 74% respectively), as efficient microprocessor based MPPT and PCS have been used and the number of switches has been reduced in ECS. Now the system can use all of the PV power since we can estimate its value beforehand. Moreover, the buy power is very smooth compared to the previous one as we can optimize this value.

In our future work, we shall try to estimate the PV output power for partially rainy/cloudy days using one day-ahead weather forecast and to develop a simulation method to calculate the optimum value of buy power automatically.

Acknowledgements

The research is being continued by the financial support of 'Grant-in-Aid for Scientific Research (14350139)' of Japan Society for the Promotion of Science (JSPS). The authors would like to express their sincere thanks to Mr. K. Mitsui and Mr. M. Shimizu of Power System Co. for their technical help.

(Manuscript received Feb. 26, 2004,
revised Oct. 29, 2004)

References

(1) R. Om, S. Yamashiro, R.K. Mazumder, K. Nakamura, K. Mitsui, M. Yamagishi, and M. Okamura: "Design and performance evaluation of grid connected PV-ECS system with load leveling function", *T. IEE Japan*, Vol.121-B, No.9, pp.1112–1119 (2001-9)

(2) S. Machida and T. Tani: "Introduction effect of the load leveling system with solar cell and storage battery", *T. IEE Japan*, Vol.122-B, No.1, pp.37–46 (2003-1) (in Japanese)

(3) M. Okamura: EDLCs and Storage System, Nikkan Kogyo Shinbun (1999) (in Japanese)

(4) J.A. Duffie and W.A. Beckman: Solar Engineering of Thermal Processes, John Willey and Sons, New York (1980)

(5) M. Okamura: "A new capacitor-electronics power storage", Proc. of EVS-13, Vol.6H-01, No.1 (1996)

(6) M. Oshima and E. Masada: "A single-phase PCS with a novel constantly sampled current-regulated PWM scheme", *IEEE Trans. Power Electronics*, Vol.14, No.5, pp.823–830 (1999-9)

Md. Habibur Rahman (Student Member) was born in Dhaka, Bangladesh, on March 10, 1970. He received his B.Sc. (Honors) degree and M.Sc. degree in 1994 and 1996 respectively from the Dept. of Applied Physics and Electronics, the University of Dhaka, Bangladesh. He is an Assistant Professor in the same department. Now he is working as a Ph.D. student in Kitami Institute of Technology, Japan. His research work concerns distributed generation system and photovoltaic. He is a student member of IEEJ and a member of BASSP and Bangladesh Electronic Society.

Susumu Yamashiro (Senior Member) received his B.E, M.E. and Dr. Eng. from Hokkaido University in 1963, 1965 and 1967 respectively. In 1971, he joined Kitami Institute of Technology as an associate professor and become a professor of the Department of Electrical and Electronic Engineering in 1978 where he is currently working. In 1979, he was a visiting professor at Purdue University, U.S.A., and University of London, U.K. His research mainly concerns the power system engineering. He is a member of Japan Solar Energy Society, the Institute of Electrical Facility Engineers of Japan, and the Thermal and Nuclear Power Engineering Society. He is also a member of IEEE.

Koichi Nakamura (Member) received his Bachelor Degree in Electrical Engineering (B.E) from Kitami Institute of Technology in 1980. At the same year, he joined the Kitami Institute of Technology as a technical associate and then become assistance professor in 1994. His research mainly concerns on an evaluation of a power system planning, the development of new type of energy storage devices and the evaluation of the photovoltaic system for residences. He is a member of Japan Solar Energy Society.